

Facile Chemical Synthesis of Pure Cu doped CeO₂ Nanoparticles: Evaluation of Fundamental Properties and Photocatalytic Activity on Rhodamine B Dye

SWATHI CHIDARABOYINA^{1,2}, ARPUTHARAJ SAMSON NESARAJ^{1,3,*} and MANASAI ARUNKUMAR¹

¹Department of Applied Chemistry, Karunya Institute of Technology and Sciences (Deemed to be University), Karunya Nagar, Coimbatore-641114, India

²Department of Chemistry, Keshav Memorial Institute of Technology, 3-5-1026, Narayanaguda, Hyderabad-500029, India

³Department of Chemistry, School of Advanced Sciences, Kalasalingam Academy of Research and Education (Deemed to be University), Anand Nagar, Krishnankoil-626126, India

*Corresponding author: E-mail: samson@klu.ac.in

Received: 13 June 2022;

Accepted: 31 August 2022;

Published online: 25 November 2022;

AJC-21031

Copper doped CeO₂ (Ce_{1-x}Cu_xO_{2.8}; x = 0.10, 0.20, 0.30, 0.40 and 0.50) nanoparticles were synthesized by wet chemical precipitation process. These materials were characterized by XRD, FTIR, EDAX, SEM, UV and photoluminescence spectroscopic techniques. These samples exhibited FCC crystalline structure. The FTIR showed the presence of Ce-O vibration in the prepared samples, whereas SEM exhibited smaller and bigger grains in the materials. The band gap energy (E_g) was measured in the range of 1.5-3 eV. The photoluminescence spectra for all the suspensions were obtained in the range of 390 to 550 nm. The photocatalytic elimination of Rhodamine B in the presence of Ce_{1-x}Cu_xO_{2.8} nano-photocatalysts under UV light was studied. The highest photodegradation efficiency (68.05%) was found at pH = 11 after 60 min irradiation in UV light at room temperature for Ce_{0.90}Cu_{0.10}O_{2.8}.

Keywords: Cu doped CeO₂ nanoparticles, Rhodamine B, Dye removal, Photocatalytic degradation, UV irradiation.

INTRODUCTION

Dyeing agents are coloured compounds which are dissolved in a liquid to give off a certain colour *via* scattering of light or selective absorption [1]. The development of textile industry increases the environment contamination due to dye pollutants. These hazardous chemicals released from industries through wastewater have high toxicity with slow biodegradation characteristics [2,3]. The removal of organic and inorganic compounds from industrial effluents is expensive. The chemical treatment like photocatalysis is a low cost and high effective process compared to other purification methods [4,5]. In photocatalytic degradation process, variety of toxic organic pollutants would be oxidized to carbon dioxide, water and harmless compounds [6]. The photocatalysis involves the mechanism to produce an electron/hole pair using light source. It was reported that the nanomaterials based photocatalysts have high surface energy along-with high surface-to-volume ratio, which help them to exhibit high degradation efficiency in removing the dyes under UV or visible light irradiation from water [7].

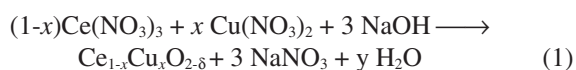
Nano CeO₂ has a remarkable feature of chemical stability with a wide band gap and low toxicity. Hence, it is used in various fields, such as biomedical, electrolyte in solid oxide fuel cell, oxidation of the volatile organic compounds and photocatalysts in wastewater treatment technology [8,9]. Yttrium doped CeO₂ photocatalyst exhibited a best performance in eliminating Rhodamine B dye under visible radiation [10]. Sol-gel prepared Ca doped CeO₂ quantum dots showed high photodegradation efficiency (84%) to degrade methylene blue dye using sunlight [11]. Rhodamine 6G dye was degraded by N-doped CeO₂ microspheres with high photocatalytic degradation using visible light ($\lambda > 420$ nm) irradiation [12]. Sm-doped CeO₂ (SC) showed high photooxidation activity than undoped CeO₂ in removing the organic pollutants, *viz.* bisphenol A (BPA) acetaldehyde, respectively [13]. The azo dye acid orange 7 (AO7) was degraded by Co-doped cerium and showed good photocatalytic activity in aqueous solution under UV irradiation [14]. Malachite green was degraded by V doped CeO₂ with alkali-activated steel slag-based nanocomposite and exhibited high photodegradation under UV light illumination [15].

Rhodamine B (RhB) is a dye with molecular weight 479.01, which could exhibit good absorption peak in visible region of electromagnetic spectrum (554 nm) with more stability at various pH values. NaBiO₃ was efficient in degrading the RhB dye under visible light within 30 min under a given set of conditions [16]. The RhB causes damage to the human cells and tissues in less time [17]. Hence, it is important to find suitable ways to remove this dye from water. The present work is dealt with the synthesis and characterization of Cu doped CeO₂ (Ce_{1-x}Cu_xO_{2.8}; $x = 0, 0.1, 0.2, 0.3, 0.4, 0.5$) nanoparticles by simple chemical precipitation method and characterized by different analytical tools. The photocatalytic performance characteristics of Cu doped CeO₂ nanoparticles in removing the RhB dye from water under UV light illumination is also investigated.

EXPERIMENTAL

Cerium nitrate hexahydrate (98%, SRL, India), cupric nitrate trihydrate (95%, Loba Chemie, India), sodium hydroxide (97%, Merck, India) and ethanol (99.9%, CS, China) were used for the preparation of nanoparticles using double distilled water.

Synthesis of Cu doped CeO₂ nanoparticles by simple chemical precipitation: Metal nitrate salts (Mⁿ⁺ = Ce³⁺ and Cu²⁺) with appropriate stoichiometric ratio (Table-1) were dissolved in 10 mL of double distilled water. From burette, NaOH solution of appropriate concentration was added dropwise to the beaker containing metal nitrate solution and mixed well to complete the precipitation reaction. With the addition of NaOH flakes, the solution pH was maintained above 9. This mixture was stirred using magnetic stirrer at 800 rpm for 2 h at room temperature. The precipitate mixture [Ce(OH)₃ + Cu(OH)₂] was filtered off using Büchner funnel and washed thoroughly with 9:1 ratio of water-ethanol mixture. This purified material was stored in an oven to 60 °C for 2 h and dried followed by heat treatment at different temperatures *viz.* 150, 300, 450 and 600 °C for 2 h each resulting in the formation of fine pure Cu doped CeO₂ (Ce_{1-x}Cu_xO_{2.8}, where $x = 0, 0.1, 0.2, 0.3, 0.4$ and 0.5) nanoparticles. The synthetic methodology can be indicated *via* a chemical equation as shown in eqn. 1:



where $x = 0, 0.1, 0.2, 0.3, 0.4$ and 0.5.

TABLE-1

AMOUNT OF PRECURSOR SALTS USED FOR THE SYNTHESIS OF CeO₂ AND Cu DOPED CeO₂ NANOPARTICLES [VOLUME OF EACH SOLUTION IS 10 mL]

Sample	Weight of Ce(NO ₃) ₃ (g)	Weight of Cu(NO ₃) ₂ (g)	Weight of NaOH (g)
CeO ₂	4.342	-	1.6
Ce _{0.90} Cu _{0.10} O _{2.8}	3.907	0.120	1.6
Ce _{0.80} Cu _{0.20} O _{2.8}	3.473	0.483	1.6
Ce _{0.70} Cu _{0.30} O _{2.8}	3.039	0.724	1.6
Ce _{0.60} Cu _{0.40} O _{2.8}	2.605	0.966	1.6
Ce _{0.50} Cu _{0.50} O _{2.8}	2.171	1.208	1.6

Characterization: The crystalline properties of parent CeO₂ and Cu doped CeO₂ nanoparticles were determined by

XRD technique (Shimadzu XRD 6000) with CuK α radiation ($K = 0.154059$ nm). The DOS computer programming was used to measure the unit cell parameter and with the help of Debye-Scherrer's formula, the average crystallite size for the samples was determined. FTIR spectra were recorded by FTIR spectrometer (IR Prestige 21) to determine the functional groups present in the samples. The surface phenomena and compositional analysis were studied by SEM (JEOL JSM-6610) instrument attached with EDAX facility at 20 kV. The UV-Vis spectral studies were carried-out by UV-spectrophotometer (Shimadzu 1800).

Photocatalytic experiment: Rhodamine B dye was used in this experiment to study the photocatalytic performance of Cu doped CeO₂ nanoparticles. For each experiment, 50 mL of RhB dye (0.005 g of RhB dye dissolved in 1 L of double distilled water) was mixed with certain amount of catalyst (0.02 g of Cu doped CeO₂ nanoparticles) for 30 min in dark to attain absorption equilibrium. Then, the sample was irradiated to the UV light and stirred for 1 h. The sampling was performed at 15 min intervals (0, 15, 30, 45 and 60 min). The photoreacted solutions (3 mL) of the centrifuged samples was taken out for UV-visible spectroscopy analysis at a wavelength of 554 nm. The degradation percentage of dye was determined using eqn. 2:

$$\text{Degradation of dye (\%)} = \frac{C_0 - C_t}{C_0} \times 100 \quad (2)$$

where, C₀ is the initial absorbance of RhB dye solution and C_t is the absorbance of RhB dye solution after photodegradation for certain time 't'.

RESULTS AND DISCUSSION

XRD studies: The XRD patterns of CeO₂ and Cu doped CeO₂ nanoparticles are shown in Fig. 1. The XRD patterns are in line with the standard CeO₂ data (JCPDS card no. 65-5923). The samples were assigned to FCC crystalline structure. The 2 θ values observed at 28.46°, 32.99°, 47.41°, 56.29° and 69.35° were relevant to the *hkl* values *viz.* (111), (200), (220), (311) and (400), respectively for CeO₂ as reported in literature [18-20]. The crystallite size (D_x) was measured by using Debye-Scherrer's equation as shown in eqn. 3:

$$D_x = \frac{k\lambda}{\beta \cos \theta} \quad (3)$$

where, β is the full width at half max (FWHM) of a diffraction peak, k is the shape factor approximately 0.91, λ is the wavelength of the X-ray source (1.54 Å) and θ is the Bragg's angle. The calculated crystallite size values varied between ranges from 15.76 to 20.69 nm are shown in Table-2, which are in line with the reported data [14]. The theoretical density (D_p) was calculated by using eqn. 4:

$$D_p (\text{g cm}^{-3}) = \frac{Z \times M}{N \times V} \quad (4)$$

where, 'Z' is number of chemical species in the unit cell, 'M' is the molecular mass of the sample (g/mol), 'N' is Avagadro's number (6.023 × 10²³), 'V' is the unit cell volume (cm³) equals

TABLE-2
CRYSTALLOGRAPHIC PARAMETERS OBTAINED ON CeO₂ AND Cu DOPED CeO₂ NANOPARTICLES

Sample	Crystal structure	Unit cell parameter (Å)	Unit cell volume (Å ³)	Crystallite size (nm)	Theoretical density (g cm ⁻³)
CeO ₂	Cubic (F.C)	5.39	156.59	20.69	7.30
Ce _{0.90} Cu _{0.10} O _{2.8}	Cubic (F.C)	5.41	158.42	20.94	6.86
Ce _{0.80} Cu _{0.20} O _{2.8}	Cubic (F.C)	5.40	157.46	21.34	6.59
Ce _{0.70} Cu _{0.30} O _{2.8}	Cubic (F.C)	5.41	158.42	21.81	6.23
Ce _{0.60} Cu _{0.40} O _{2.8}	Cubic (F.C)	5.40	157.46	17.44	5.94
Ce _{0.50} Cu _{0.50} O _{2.8}	Cubic (F.C)	5.43	160.10	15.76	5.53

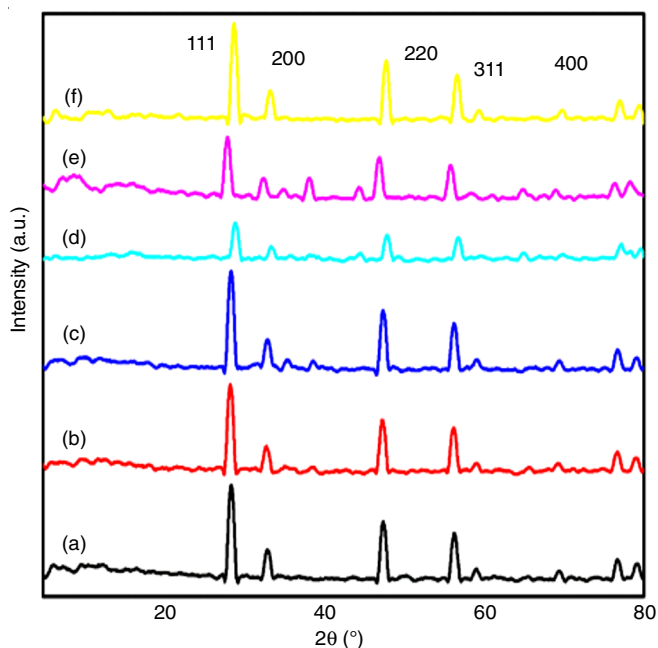


Fig. 1. XRD spectra of CeO₂ based nanoparticles (a) Pure CeO₂; (b) Ce_{0.90}Cu_{0.10}O_{2.8}; (c) Ce_{0.80}Cu_{0.20}O_{2.8}; (d) Ce_{0.70}Cu_{0.30}O_{2.8}; (e) Ce_{0.60}Cu_{0.40}O_{2.8}; (f) Ce_{0.50}Cu_{0.50}O_{2.8}

to 'a³' (where 'a' is the lattice constant in cm). The theoretical density of the materials is in between 5.53 to 7.30 g/cc.

FTIR studies: The FTIR spectra of CeO₂ and Cu doped CeO₂ nanoparticles are shown in Fig. 2. The peaks appeared at 3440 to 3460 cm⁻¹ attributed to OH stretching vibration because of the presence of adsorbed water on the surface CeO₂ nanoparticles [21,22]. The peak at 1632 cm⁻¹ attributed to the H-O-H bending vibration and the absorption band at 416 to 450 cm⁻¹ relevant to the Cu-O stretching mode of the vibration whereas the peak found at 1020 cm⁻¹ relevant to the Ce-O stretching mode of the vibration as reported [23].

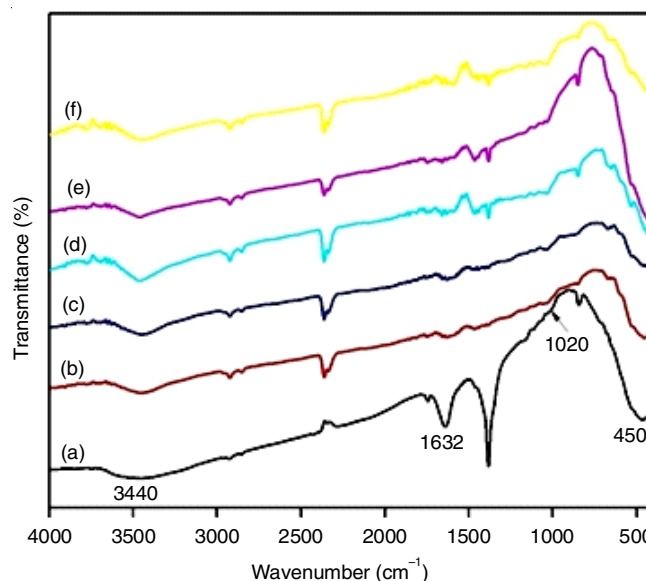


Fig. 2. FTIR spectra of CeO₂ based nanoparticles (a) Pure CeO₂; (b) Ce_{0.90}Cu_{0.10}O_{2.8}; (c) Ce_{0.80}Cu_{0.20}O_{2.8}; (d) Ce_{0.70}Cu_{0.30}O_{2.8}; (e) Ce_{0.60}Cu_{0.40}O_{2.8}; (f) Ce_{0.50}Cu_{0.50}O_{2.8}

Elemental analysis: The elemental analysis of CeO₂ and Cu doped CeO₂ nanoparticles was carried out by EDAX spectral analysis. The presence of appropriate atomic weight percentage of Ce, Cu and O was confirmed in the samples by EDAX results (Fig. 3). The elemental data of all the samples is shown in Table-3.

SEM studies: From the SEM images (Fig. 4), it was observed that the grain size of the samples is varied between 200 nm to ~500 nm. The occurrence of bigger grains in the sample is due to agglomeration effect of high temperature heat treatment. It was reported that the nanoparticles having varied grain size and random distribution pattern can result in excellent photocatalytic behavior [24]. During the calcination process, suitable

TABLE-3
ELEMENTAL COMPOSITION DATA OBTAINED ON CeO₂ AND Cu DOPED CeO₂ NANOPARTICLES BY EDAX ANALYSIS

Sample	Cerium		Copper		Oxygen	
	Atomic (%)	Weight (%)	Atomic (%)	Weight (%)	Atomic (%)	Weight (%)
CeO ₂	26.23	75.7	—	—	73.77	24.30
Ce _{0.90} Cu _{0.10} O _{2.8}	22.73	71.06	1.29	1.82	75.98	27.12
Ce _{0.80} Cu _{0.20} O _{2.8}	16.73	60.05	4.77	7.76	78.5	32.18
Ce _{0.70} Cu _{0.30} O _{2.8}	15.94	55.98	8.67	13.8	75.39	30.23
Ce _{0.60} Cu _{0.40} O _{2.8}	19.09	60.1	10.13	14.46	70.78	25.44
Ce _{0.50} Cu _{0.50} O _{2.8}	15.15	51.32	13.78	21.18	71.07	27.50

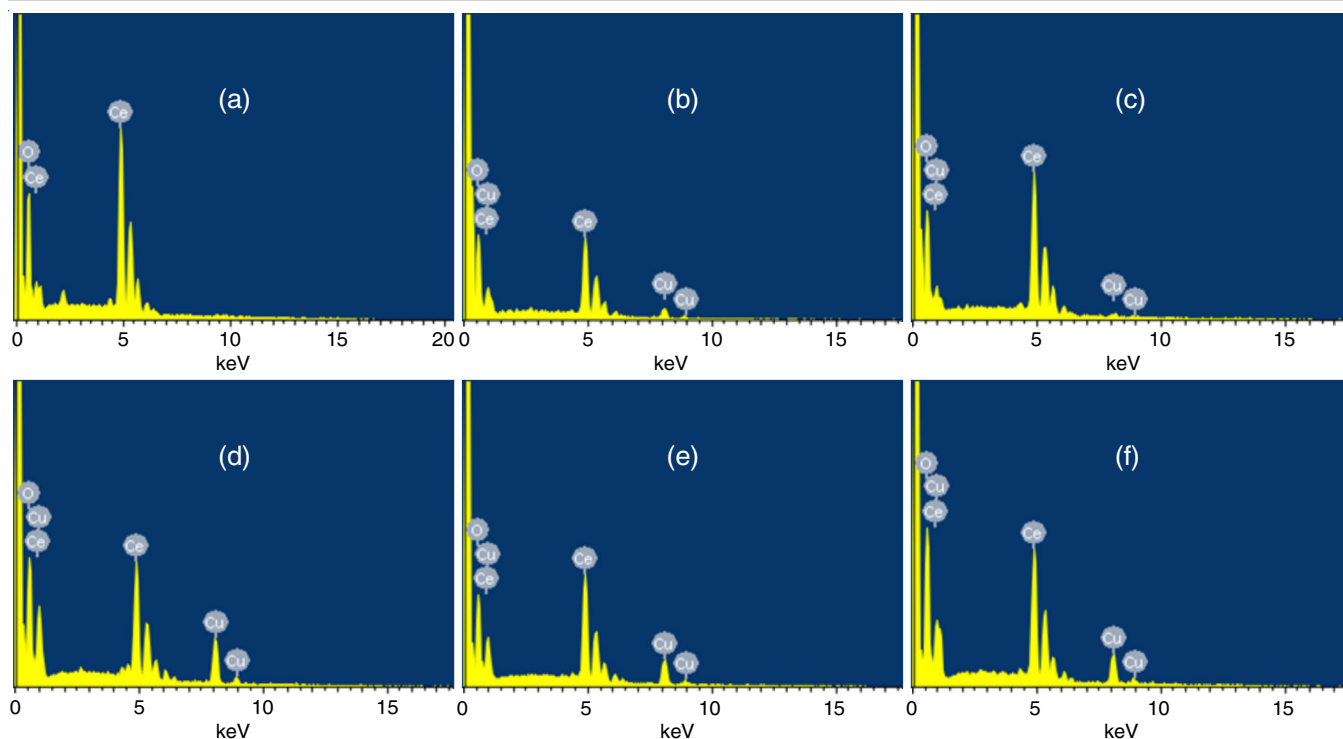


Fig. 3. EDAX spectra of CeO₂ based nanoparticles (a) Pure CeO₂; (b) Ce_{0.90}Cu_{0.10}O_{2-δ}; (c) Ce_{0.80}Cu_{0.20}O_{2-δ}; (d) Ce_{0.70}Cu_{0.30}O_{2-δ}; (e) Ce_{0.60}Cu_{0.40}O_{2-δ}; (f) Ce_{0.50}Cu_{0.50}O_{2-δ}

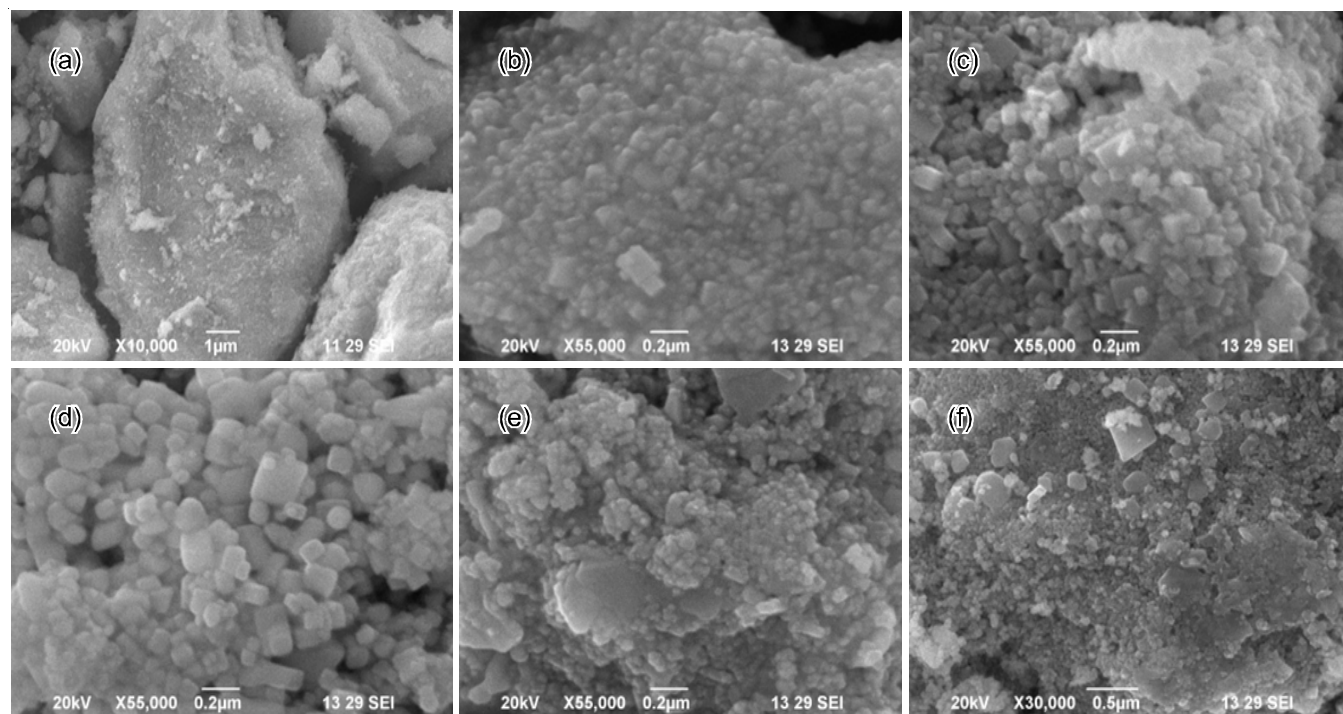


Fig. 4. SEM images of CeO₂ based nanoparticles (a) Pure CeO₂; (b) Ce_{0.90}Cu_{0.10}O_{2-δ}; (c) Ce_{0.80}Cu_{0.20}O_{2-δ}; (d) Ce_{0.70}Cu_{0.30}O_{2-δ}; (e) Ce_{0.60}Cu_{0.40}O_{2-δ}; (f) Ce_{0.50}Cu_{0.50}O_{2-δ}

heating rate should be adopted which can control the grain structure in the materials as reported [25].

UV studies: From the UV-visible spectra (Fig. 5), it is found that pure and Cu doped CeO₂ nanoparticles showed a strong absorption peak at 342 nm. It was reported that Ce(III) can exhibit absorption in UV and visible region while Ce(IV) can show absorption in the visible region only [26]. The

absorption energy band gap (E_g) was calculated using Tauc equation (eqn. 5).

$$(\alpha h\nu)^n = A(h\nu - E_g) \quad (5)$$

where ' α ' is the absorption coefficient, ' $h\nu$ ' is the energy of induced photons, ' A ' is proportionality constant, ' h ' is the Planck's constant, ' ν ' is the frequency of vibration, and exponent ' n ' is

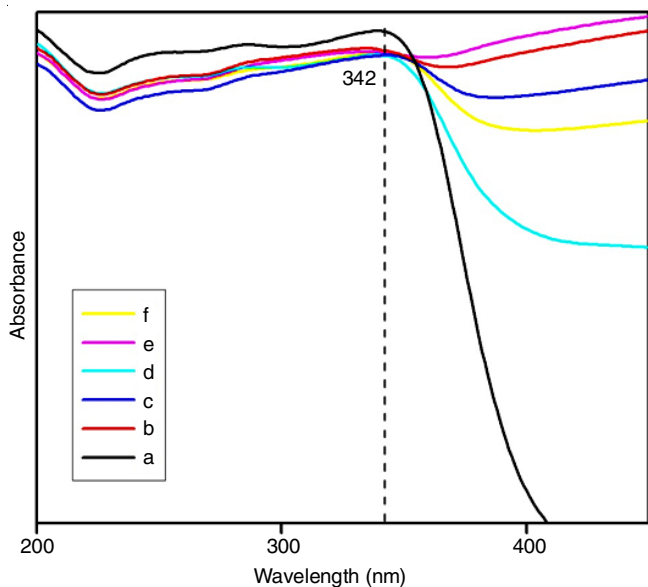


Fig. 5. UV-visible spectra obtained on CeO₂ based nanoparticles (a) Pure CeO₂; (b) Ce_{0.90}Cu_{0.10}O_{2.8}; (c) Ce_{0.80}Cu_{0.20}O_{2.8}; (d) Ce_{0.70}Cu_{0.30}O_{2.8}; (e) Ce_{0.60}Cu_{0.40}O_{2.8}; (f) Ce_{0.50}Cu_{0.50}O_{2.8}

either 2 for direct band transitions or $\frac{1}{2}$ for indirect band transitions. The absorption coefficient (α) has been calculated using the relation $\alpha = 2.303 (A/t)$, where 't' is thickness and 'A' is optical absorbance [27]. An extrapolation of the linear portion of a plot of $(\alpha hv)^2$ with hv gives the value of the optical band gap (E_g) as shown in Fig. 6. The band gap was found to be 3.0 eV using Tauc equation for pure CeO₂ and the band gap was in the range of 1.5 to 2.7 eV for the CeO₂ samples doped with Cu. Similar kind of behaviour was reported for Co-doped nanocrystals of CeO₂ with band gap of 1.61 eV [28].

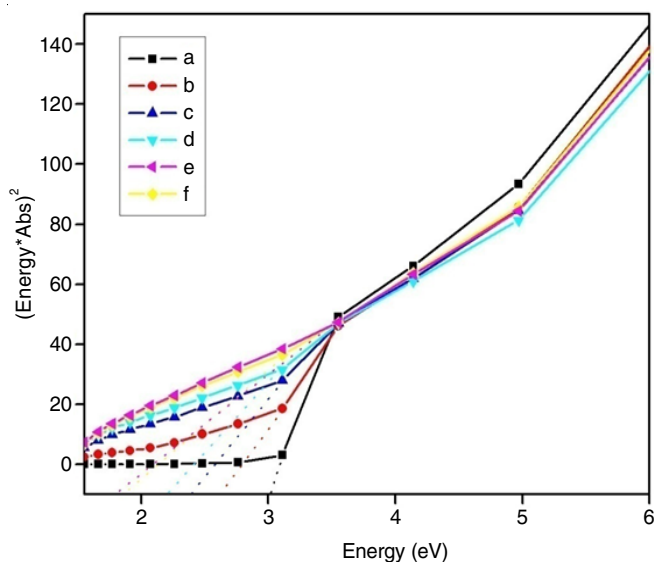


Fig. 6. Band gap curves obtained on CeO₂ based nanoparticles (a) Pure CeO₂; (b) Ce_{0.90}Cu_{0.10}O_{2.8}; (c) Ce_{0.80}Cu_{0.20}O_{2.8}; (d) Ce_{0.70}Cu_{0.30}O_{2.8}; (e) Ce_{0.60}Cu_{0.40}O_{2.8}; (f) Ce_{0.50}Cu_{0.50}O_{2.8}

Photoluminescence studies: The photoluminescence (PL) spectra obtained on undoped and Cu doped CeO₂ nanoparticles are shown in Fig. 7. It was reported that the PL emission

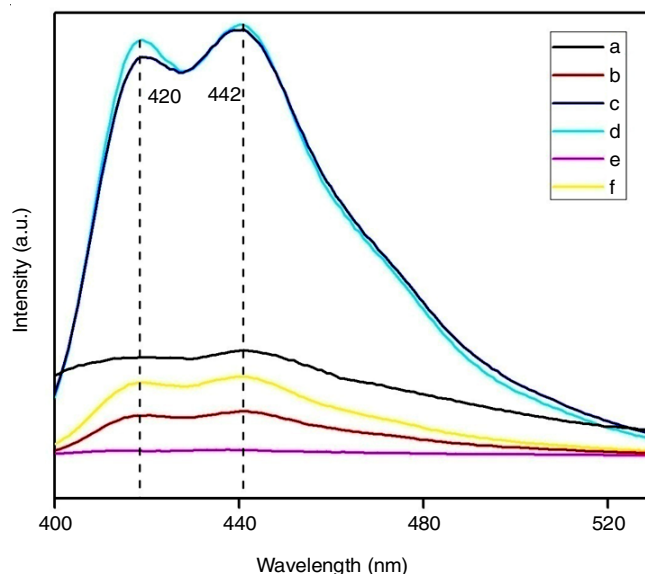


Fig. 7. Photoluminescence spectra obtained on CeO₂ based nanoparticles (a) Pure CeO₂; (b) Ce_{0.90}Cu_{0.10}O_{2.8}; (c) Ce_{0.80}Cu_{0.20}O_{2.8}; (d) Ce_{0.70}Cu_{0.30}O_{2.8}; (e) Ce_{0.60}Cu_{0.40}O_{2.8}; (f) Ce_{0.50}Cu_{0.50}O_{2.8}

depends on the presence of Cu in the synthesized samples which may lead to changes in the material disorders and defects [29]. The peaks found in Fig. 7 revealed the crystalline behavior of CeO₂ based nanoparticles [30]. The samples exhibited two peaks, the first peak at 420 nm (blue emission) and the second peak at 442 nm (blue emission). These phenomena of samples may be due to the structural characteristics of the materials. Based on the above PL results, for further photodegradation experiments, UV light source has been utilized.

Photocatalytic studies: The photocatalytic elimination activity of RhB dye was carried out using parent CeO₂ and Cu doped CeO₂ nanophotocatalysts. Fig. 8 shows the photocatalytic degradation curves obtained in this experiment. The results revealed that the optimum photocatalytic efficiency (36.7%) was shown by Ce_{0.90}Cu_{0.10}O_{2.8} after 60 min of UV irradiation compared to the other compositions. This is mainly because of the presence of more amount of Cu which might diminish the photocatalyst efficiency [31,32]. Thus, 10% Cu doped CeO₂ based nanophotocatalyst (Ce_{0.90}Cu_{0.10}O_{2.8}) was used further as an optimized material for studying the photocatalysis with respect to effect of pH and dye concentration.

A plot drawn between $\ln C_t/C_0$ vs. time is shown in Fig. 9. The slope of the straight line resulted as a first order rate constant (k). From Langmuir and Hinshelwood kinetic model (eqn. 6), the photocatalytic reaction obeyed the mechanism of pseudo first order [33].

$$\ln \frac{C_t}{C_0} = -kt \quad (6)$$

where 'C₀' is the initial concentration, 'C_t' is the concentration after time 't' and 'k' is the first order rate constant. The rate constant values were found to be 0.08 min⁻¹ (CeO₂), 0.0046 min⁻¹ (Ce_{0.90}Cu_{0.10}O_{2.8}), 0.005 min⁻¹ (Ce_{0.80}Cu_{0.20}O_{2.8}), 0.007 min⁻¹ (Ce_{0.70}Cu_{0.30}O_{2.8}), 0.006 min⁻¹ (Ce_{0.60}Cu_{0.40}O_{2.8}) and 0.001 min⁻¹ (Ce_{0.50}Cu_{0.50}O_{2.8}). During the degradation of contaminants

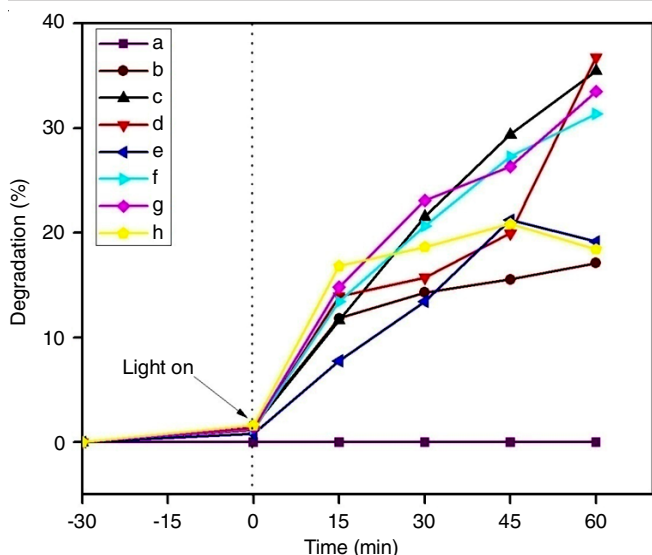


Fig. 8. Photodegradation curves obtained in presence of CeO_2 based nanophotocatalysts with Rhodamine B dye and Rhodamine B dye alone without nanophotocatalysts (a) Rhodamine B alone in dark, (b) Rhodamine B alone in light, (c) Pure CeO_2 ; (d) $\text{Ce}_{0.90}\text{Cu}_{0.10}\text{O}_{2.8}$; (e) $\text{Ce}_{0.80}\text{Cu}_{0.20}\text{O}_{2.8}$; (f) $\text{Ce}_{0.70}\text{Cu}_{0.30}\text{O}_{2.8}$; (g) $\text{Ce}_{0.60}\text{Cu}_{0.40}\text{O}_{2.8}$; (h) $\text{Ce}_{0.50}\text{Cu}_{0.50}\text{O}_{2.8}$

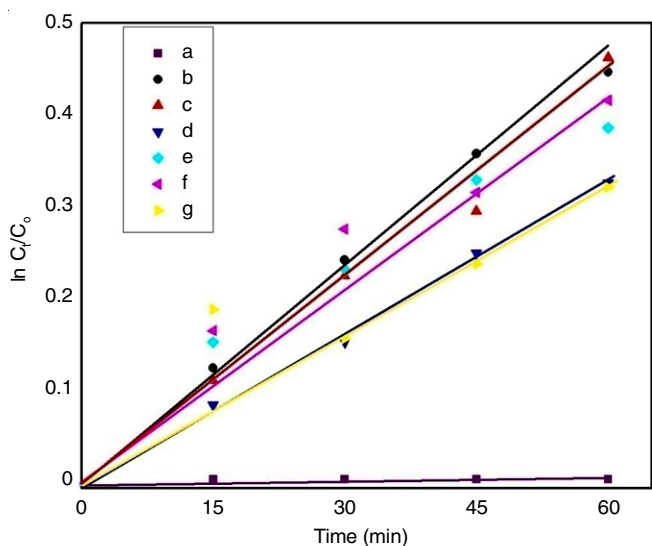


Fig. 9. First order kinetic plot of Rhodamine B dye using (a) Rhodamine B alone in the absence of photocatalyst; (b) Pure CeO_2 ; (c) $\text{Ce}_{0.90}\text{Cu}_{0.10}\text{O}_{2.8}$; (d) $\text{Ce}_{0.80}\text{Cu}_{0.20}\text{O}_{2.8}$; (e) $\text{Ce}_{0.70}\text{Cu}_{0.30}\text{O}_{2.8}$; (f) $\text{Ce}_{0.60}\text{Cu}_{0.40}\text{O}_{2.8}$; (g) $\text{Ce}_{0.50}\text{Cu}_{0.50}\text{O}_{2.8}$

using photocatalysts, the photoexcitation of CeO_2 in aqueous solution results in the formation of various radicals and charged species (eqns. 7-10) [34]:



where $h\nu$ denotes the energy of induced photons, VB is the valence band in CeO_2 , CB represents the conduction band in CeO_2 , hole is represented by h^+ and an electron is represented by e^- .

Effect of pH: To enhance the photocatalytic performance of the material, the parameter of changing of pH can be used [35]. By varying the pH of the dye solution with photocatalysts, the photodegradation efficiency was measured after irradiation in UV light source after 1 h. Dilute HCl and dilute NaOH were added to the dye solution for the acidic and basic pH environment. For this study, pH values, *viz.* 2.5, 4.3, 6.5, 9.0 and 11.0 were fixed. The photocatalytic efficiency of $\text{Ce}_{0.90}\text{Cu}_{0.10}\text{O}_{2.8}$ towards RhB dye due to the effect of pH is shown in Fig. 10. The optimum photodegradation efficiency (68.05%) was observed at pH = 11 in comparison with other pH values. It was observed that the maximum degradation is favourable at alkaline medium compared to low pH range. Depending on the variation of pH, the CeO_2 nanoparticles can behave as either positively or negatively charge [36]. The optimum RhB degradation at pH 11 can be due to the more attributed rate of photocatalysis of nanophotocatalyst [37].

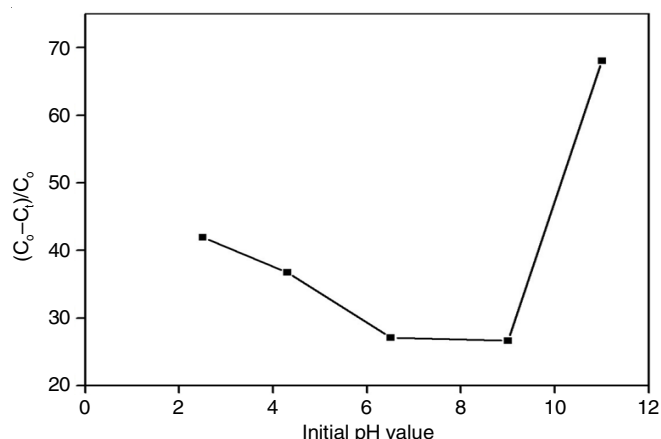


Fig. 10. Effect of pH value on the degradation efficiency of Rhodamine B using $\text{Ce}_{0.90}\text{Cu}_{0.10}\text{O}_{2.8}$ photocatalyst material

Effect of initial concentration of dye: The photocatalytic efficiency of the best performing material ($\text{Ce}_{0.90}\text{Cu}_{0.10}\text{O}_{2.8}$) was studied further at a standardized pH = 11 along-with RhB dye having different concentrations, *viz.* 0.0025, 0.005, 0.0075 and 0.01 g/L after 60 min of UV irradiation. The effect of initial concentration of RhB dye on the photocatalytic efficiency of $\text{Ce}_{0.90}\text{Cu}_{0.10}\text{O}_{2.8}$ (best sample) is shown in Fig. 11. Among the

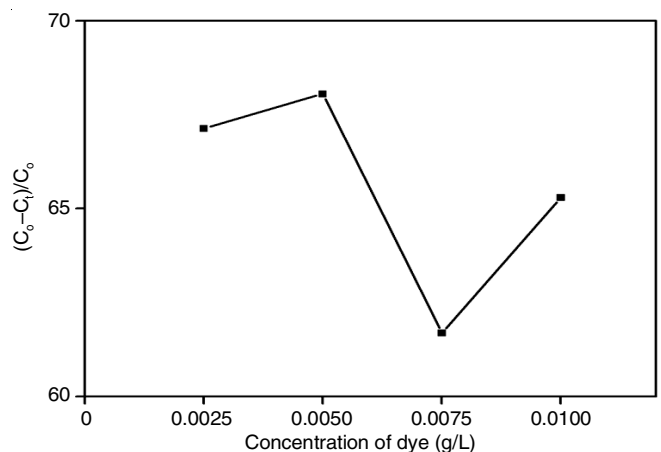


Fig. 11. Effect of Rhodamine B dye concentration on the photocatalytic efficiency of $\text{Ce}_{0.90}\text{Cu}_{0.10}\text{O}_{2.8}$

various concentration studied, the optimum photocatalytic efficiency was reported to be 68% with the dye concentration of 0.005 g/L at pH 11. It was reported that the initial concentration of dye plays a potential role in the photocatalytic elimination. When the concentration of RhB enhanced, it resulted in lower photocatalytic efficiency. However, at an optimum concentration of 0.005 g/L of RhB, the light penetration might be more, which exhibited high photocatalytic efficiency as reported. The path length of photons present in the solution might be increased at this concentration of dye solution [38].

Conclusion

Pure CeO₂ and Cu doped CeO₂ (Ce_{1-x}Cu_xO_{2-δ}; where $x = 0, 0.10, 0.20, 0.30, 0.40$ and 0.50) nanoparticles were prepared by facile chemical synthesis. The XRD data revealed the FCC crystalline structure for all the samples. Further, the functional, elemental, morphological and optical properties of CeO₂ and Cu doped CeO₂ nanoparticles were analyzed by performing FTIR, EDAX, SEM, UV-visible and photoluminescence characterizations. The UV-visible spectra showed a strong absorption peak around 342 nm (λ_{max}) in all the composition of CeO₂ samples. The band gap energy (E_g) of Ce_{1-x}Cu_xO_{2-δ} was found to be in the range of 1.5-3 eV. The photoluminescence spectra of samples showed 2 peaks, viz. at 420 nm (blue emission) and the other at 442 nm (blue emission). Among the different compositions of Cu doped CeO₂ studied, Ce_{0.90}Cu_{0.10}O_{2-δ} resulted in the excellent performance towards degradation of Rhodamine B dye with 68.05% of efficiency using ultraviolet illumination. The degradation efficiency was found to be maximum at pH 11 at an optimum concentration of 0.005 g/L of Rhodamine B dye.

ACKNOWLEDGEMENTS

The authors thank Karunya Institute of Technology and Sciences (KITS) for providing the necessary research facilities to complete this research activity.

CONFLICT OF INTEREST

The authors declare that there is no conflict of interests regarding the publication of this article.

REFERENCES

- Z. Hao and A. Iqbal, *Chem. Soc. Rev.*, **26**, 203 (1997); <https://doi.org/10.1039/cs9972600203>
- M. Qamar and M. Muneer, *Desalination*, **249**, 535 (2009); <https://doi.org/10.1016/j.desal.2009.01.022>
- D.G.J. Larsson, C. de Pedro and N. Paxeus, *J. Hazard. Mater.*, **148**, 751 (2007); <https://doi.org/10.1016/j.jhazmat.2007.07.008>
- S. Werle and M. Dudziak, *Energies*, **7**, 462 (2014); <https://doi.org/10.3390/en7010462>
- H. Zhou, Y. Qu, T. Zeid and X. Duan, *Energy Environ. Sci.*, **5**, 6732 (2012); <https://doi.org/10.1039/C2EE03447F>
- G. Ren, H. Han, Y. Wang, S. Liu, J. Zhao, X. Meng and Z. Li, *Nanomaterials*, **11**, 1804 (2021); <https://doi.org/10.3390/nano11071804>
- Y. Li, W. Wang, F. Wang, L. Di, S. Yang, S. Zhu, Y. Yao, C. Ma, B. Dai and F. Yu, *Nanomaterials*, **9**, 720 (2019); <https://doi.org/10.3390/nano9050720>
- M. Murugalakshmi, B.F. Jones, G. Mamba, D. Maruthamani and V. Muthuraj, *New J. Chem.*, **45**, 4046 (2021); <https://doi.org/10.1039/D0NJ04844E>
- B. Samai and S.C. Bhattacharya, *Mater. Chem. Phys.*, **220**, 171 (2018); <https://doi.org/10.1016/j.matchemphys.2018.08.050>
- A. Akbari-Fakhrabadi, R. Saravanan, M. Jamshidijam, R.V. Mangalaraja and M.A. Gracia, *J. Saudi Chem. Soc.*, **19**, 505 (2015); <https://doi.org/10.1016/j.jscs.2015.06.003>
- V. Ramasamy, V. Mohana and V. Rajendran, *OpenNano*, **3**, 38 (2018); <https://doi.org/10.1016/j.onano.2018.04.002>
- C. Wu, *Mater. Lett.*, **139**, 382 (2015); <https://doi.org/10.1016/j.matlet.2014.10.127>
- B. Xu, H. Yang, Q. Zhang, S. Yuan, A. Xie, M. Zhang and T. Ohno, *ChemCatChem*, **12**, 2638 (2020); <https://doi.org/10.1002/cctc.201902309>
- N.S. Arul, D. Mangalaraj, P.C. Chen, N. Ponpandian, P. Meena and Y. Masuda, *J. Sol-Gel Sci. Technol.*, **64**, 515 (2012); <https://doi.org/10.1007/s10971-012-2883-7>
- L. Kang, Y.J. Zhang, M.Y. Yang, L. Zhang, K. Zhang and W.L. Zhang, *Integr. Ferroelectr.*, **170**, 1 (2016); <https://doi.org/10.1080/10584587.2016.1165572>
- K. Yu, S. Yang, H. He, C. Sun, C. Gu and Y. Ju, *J. Phys. Chem. A*, **113**, 10024 (2009); <https://doi.org/10.1021/jp905173e>
- D.R. Sulistina and S. Martini, *J. Public Health Res.*, **9**, 1812 (2020); <https://doi.org/10.4081/jphr.2020.1812>
- D.M.D.M. Prabaharan, K. Sadaiyandi, M. Mahendran and S. Sagadevan, *Mater. Res.*, **19**, 478 (2016); <https://doi.org/10.1590/1980-5373-MR-2015-0698>
- J. Calvache-Muñoz, F.A. Prado and J.E. Rodríguez-Páez, *Colloids Surf. A Physicochem. Eng. Asp.*, **529**, 146 (2017); <https://doi.org/10.1016/j.colsurfa.2017.05.059>
- A. Miri and M. Sarani, *Ceram. Int.*, **44**, 12642 (2018); <https://doi.org/10.1016/j.ceramint.2018.04.063>
- V. Ramasamy, V. Mohana and G. Suresh, *Int. J. Mater. Sci.*, **12**, 79 (2017).
- X. Guo, L. Liu, J. Wu, J. Fan and Y. Wu, *RSC Adv.*, **8**, 4214 (2018); <https://doi.org/10.1039/C7RA09894D>
- K.K. Babitha, A. Sreedevi, K.P. Priyanka, B. Sabu and T. Varghese, *Indian J. Pure Appl. Phys.*, **53**, 596 (2015).
- N. Saikumari, S.M. Dev and S.A. Dev, *Sci. Rep.*, **11**, 1734 (2021); <https://doi.org/10.1038/s41598-021-80997-z>
- R.A.M. Napitupulu, *IOP Conf. Series: Mater. Sci. Eng.*, **237**, 012038 (2017); <https://doi.org/10.1088/1757-899X/237/1/012038>
- D. Girija, H.S. Bhojya Naik, C.N. Sudhamani and B.V. Kumar, *Arch. Appl. Sci. Res.*, **3**, 373 (2011).
- S.W. Balogun, Y.K. Sansui and A.O. Aina, *Int. J. Dev. Res.*, **8**, 18486 (2018).
- T.S. Wu, Y.W. Chen, S.C. Weng, C.N. Lin, C.H. Lai, Y.J. Huang, H.T. Jeng, S.L. Chang and Y.L. Soo, *Sci. Rep.*, **7**, 4715 (2017); <https://doi.org/10.1038/s41598-017-05046-0>
- R.C. Deus, J.A. Cortés, M.A. Ramirez, M.A. Ponce, J. Andres, L.S.R. Rocha, E. Longo and A.Z. Simões, *Mater. Res. Bull.*, **70**, 416 (2015); <https://doi.org/10.1016/j.materresbull.2015.05.006>
- M.M.J. Sadiq and A.S. Nesaraj, *J. New Technol. Mater.*, **3**, 14 (2013).
- B. Xu, R.G. Song, P.H. Tang, J. Wang, G.Z. Chai, Y.Z. Zhang and Z.Z. Ye, *Key Eng. Mater.*, **373-374**, 346 (2008); <https://doi.org/10.4028/www.scientific.net/KEM.373-374.346>
- W.T. Nichols, T. Sasaki and N. Koshizaki, *J. Appl. Phys.*, **100**, 114913 (2006); <https://doi.org/10.1063/1.2390642>
- S. Pan and X. Liu, *New J. Chem.*, **36**, 1781 (2012); <https://doi.org/10.1039/c2nj40301c>
- E. Kusmierek, *Catalysts*, **10**, 1435 (2020); <https://doi.org/10.3390/catal10121435>
- U.G. Akpan and B.H. Hameed, *J. Hazard. Mater.*, **170**, 520 (2009); <https://doi.org/10.1016/j.jhazmat.2009.05.039>
- S. Rani, M. Aggarwal, M. Kumar, S. Sharma and D. Kumar, *Water Sci.*, **30**, 51 (2016); <https://doi.org/10.1016/j.wsj.2016.04.001>
- G. Naresh, J. Malik, V. Meena and T.K. Mandal, *ACS Omega*, **3**, 11104 (2018); <https://doi.org/10.1021/acsomega.8b01054>
- O. Sacco, M. Stoller, V. Vaiano, P. Ciambelli, A. Chianese and D. Sannino, *Int. J. Photoenergy*, **2012**, 626759 (2012); <https://doi.org/10.1155/2012/626759>